Original articles

Nonlinear optical properties of single-walled carbon nanotubes/water dispersed media exposed to laser radiation with nano- and femtosecond pulse durations

P. N. Vasilevsky[1,2]✉, M. S. Savelyev[1,2,3], S. A. Tereshchenko [1,2],
S. V. Selishchev[1], A. Yu. Gerasimenko[1,2,3]

[1]National Research University of Electronic Technology,
1 Shokina pl., Zelenograd, Moscow 124498, Russian Federation

[2]Institute of Nanotechnology of Microelectronics of the Russian Academy of Sciences,
32a Leninsky pr., Moscow 119991, Russian Federation

[3]I. M. Sechenov First Moscow State Medical University,
8-2 Trubetskaya ul., Moscow 119991, Russian Federation

Abstract

The constant increase in the power of laser systems and the growth of potential fields for the application of lasers make the problem of protecting sensitive elements of electro-optical systems and visual organs from high-intensity radiation an urgent issue. Modern systems are capable of generating laser radiation in a wide range of wavelengths, durations, and pulse repetition rates. High-quality protection requires the use of a universal limiter capable of attenuating laser radiation, not causing colour distortion, and having a high transmission value when exposed to low-power radiation. For this, dispersed media based on carbon nanotubes with unique physicochemical properties can be used. Such media have constant values of their absorption coefficient and refractive index when exposed to low-intensity laser radiation and change their properties only when the threshold value is reached.

The aim of this work was the study of the nonlinear optical properties of an aqueous dispersion of single-walled carbon nanotubes exposed to nano- and femtosecond radiation. For the characterization of the studied medium, Z-scan and fixed sample location experiments were used. The optical parameters were calculated using a threshold model based on the radiation transfer equation.

As a result of the experiments, it was shown that the aqueous dispersion of single-walled carbon nanotubes is capable of limiting radiation with wavelengths from the visible and near-IR ranges: nano- (532, 1064 nm) and femtosecond (810 nm). A description of nonlinear optical effects was proposed for when a medium is exposed to radiation with a nanosecond duration due to reverse saturable absorption and two-photon absorption. When the sample exposed for a femtosecond duration the main limiting effect is spatial self-phase modulation. The calculated optical parameters can be used to describe the behaviour of dispersions of carbon nanotubes when exposed to radiation with different intensities. The demonstrated effects allow us to conclude that it is promising to use the investigated media as limiters of high-intensity laser radiation in optical systems to protect light-sensitive elements.

Keywords: Laser radiation Limiters, Nano- and femtosecond radiation, Carbon nanotubes, Reverse saturable absorption, Spatial self-phase modulation, Z-scan, Radiation transfer equation

For citation: Vasilevsky P. N., Saveliev M. S., Tereshchenko S. A., Selishchev S. V., Gerasimenko A. Yu. Nonlinear optical properties of single-walled carbon nanotubes/water dispersed media exposed to laser radiation with nano- and femtosecond pulse durations. *Kondensirovannye sredy i mezhfaznye granitsy = Condensed Matter and Interphases*. 2021;23(4): 496–506. https://doi.org/10.17308/kcmf.2021.23/3668

✉ Pavel N. Vasilevsky, e-mail: pavelvasilevs@yandex.ru

Condensed Matter and Interphases / Конденсированные среды и межфазные границы   2021;23(4): 496–506

P. N. Vasilevsky et al.   Nonlinear optical properties of single-walled carbon nanotubes/water dispersed media...

1. Introduction

Since the invention of the laser in the 50s, laser radiation has been widely used in various fields [1–3]. Devices for laser welding and cutting [4], photolithography systems [5], laser surgical and vision correction complexes [6], spectrometers for determining the chemical composition of substances [7], laser designators and range finders [8] have been actively used for several decades. Recently, laser scanning using lidars and laser communication systems has been under development [9, 10].

Most of the laser systems operate in the visible and near IR regions of radiation. This is explained by the simplicity of implementation of both the laser system (for example, Nd:YAG lasers with the generation of additional harmonics) and the photodetector equipment for detecting radiation. Silicon photodiodes are sensitive in the range from 200 nm to 1100 nm, which corresponds well to the generation wavelengths of the Nd:YAG laser (1064, 532, 355 nm, etc.) [11]. Also, laser radiation in the range of 350–1100 nm is weakly absorbed by water, which makes it possible to use lidars with these wavelengths for scanning in rainy weather and for bathymetry [12].

The development of laser technology is accompanied by an increase in the power of the used systems. High-intensity radiation can interfere with the operation of light-sensitive detectors and damage the eyes. In accordance with the ANSI Z136 international standards, radiation with a power of less than 5 mW is considered safe for the human eye if the exposure time is no more than 0.25 s. When working with more powerful radiation, protective equipment must be used.

In the case of laser scanning and ranging systems, the range of measured distances is limited by the fact that the use of high-power laser pulses can overload the photodetector in the near field. This is due to the fact that as the distance to the measured object decreases, the energy of the echo pulse increases. In such cases, optical limiters of laser radiation are used to protect the

photodetector equipment. However, limiters with a constant transmission value (such as absorption and interference filters), while protecting against strong echo pulses, attenuate the "useful" signal to the same extent, i.e. decrease the upper limit of the operating range. In addition, absorption filters have spectral selectivity, i.e. their attenuation coefficient depends on the wavelength of the incident radiation.

Chromogenic materials are able to change their optical density depending on external parameters (temperature, applied voltage, etc.), but their response rate does not ensure the limitation of nanosecond pulses or less [13–15]. Therefore, potentially the most suitable media for limiting laser radiation are nonlinear optical materials.

Nonlinear optical media are those media, the optical properties of which depend on the intensity of the incident laser radiation. Such substances are used for laser three-dimensional printing [16], nonlinear optical switches [17], and can also be used to limit the intensity of laser radiation [18]. With a low intensity of I they have high transmittance (more than 70%) and constant optical parameters, such as absorption coefficient and refractive index, and upon reaching the threshold intensity of I_{th}, they start to change their transmission due to nonlinear optical effects (Fig. 1) [19].

The nonlinear optical medium exhibits different properties depending on the type of laser radiation. When exposed to pulsed nanosecond radiation with an intensity above the threshold value, nonlinear absorption occurs in the medium [20]. This property of nonlinear optical media, in addition to limiting laser radiation, can be used in optical switches to control the signal [21], as well as to create three-dimensional biocompatible structures for the restoration of damaged tissues [22]. In the case of prolonged exposure to continuous or femtosecond radiation with a high pulse repetition rate, a change in the refractive index occurs. This change causes a change in the beam's shape due to self-focusing or self-defocusing [23].
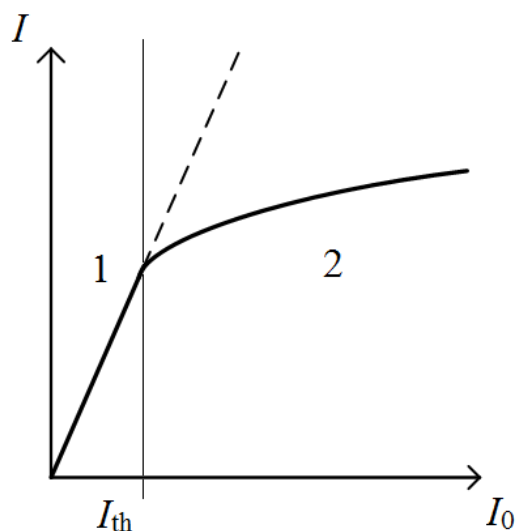
Condensed Matter and Interphases / Конденсированные среды и межфазные границы   2021;23(4): 496–506

P. N. Vasilevsky et al.   Nonlinear optical properties of single-walled carbon nanotubes/water dispersed media...

Fig. 1. Typical form of the dependence of the transmitted radiation intensity on the intensity of the incident radiation. Area *1* – linear transmission, Area *2* – nonlinear transmission

A large number of materials such as quantum dots [24], metal nanoparticles [25], organic dyes [26] and carbon nanoparticles [27] have nonlinear optical properties. Carbon nanomaterials, in contrast to dyes and metals, are colour neutral, i.e. their transmission spectrum does not have pronounced absorption peaks. By adjusting the concentration, high linear transmittance in the visible and near IR ranges can be achieved. Such a limiter can be used in tunable wavelength systems. One of the promising carbon nanomaterials are carbon nanotubes, which, in addition to optical properties exhibit unique mechanical and electrically conductive properties [28, 29].

The aim of this work was the study of the nonlinear optical properties of an aqueous dispersion of single-walled carbon nanotubes exposed to nano- and femtosecond radiation.

Samples of single-walled carbon nanotubes/water dispersion (SWCNTs) were created and experimental studies were carried out using Z-scanning methods and fixed sample location experiment. Calculations of nonlinear optical parameters, such as nonlinear absorption coefficient, nonlinear refractive index and the corresponding threshold values, allow assessing the prospects for using the investigated media as a nonlinear optical limiter.

2. Experimental

1.1. Preparation of liquid dispersions

For the production of the investigated sample, SWCNT with a purity of 95% were used. The nanotube diameter varied over the range of 1–2 nm. Distilled water with pH = 6 was used as a solvent. SWCNT were mixed with water in a way that the mass fraction of SWCNT in the initial solution did not exceed 0.005 wt%. The original solution was placed in an ultrasonic homogenizer Sonicator Q700 (Qsonica, USA), where it was stirred for 1 hour under the influence of a powerful ultrasonic field with an amplitude of 45 W. Then the aqueous dispersion was stirred on a magnetic stirrer for 1 hour.

1.2. Methods for determining the linear and nonlinear absorption

For the determination of the linear absorption coefficient, a Genesys 10S Uv-Vis single-beam spectrophotometer (Thermo Fisher Scientific, USA) was used. A xenon lamp, allowing a spectrum in the near UV, visible, and near IR ranges was used as a radiation source.

For the determination of the nonlinear absorption coefficient, an experimental system based on an LS-2147 Nd: YAG laser (LOTIS TII, Belarus) was constructed (Fig. 2). For the research the fundamental (1064 nm) and second harmonics (532 nm) were used. Irradiation was performed with single pulses. The pulse duration was 16 ns. The radiation generated by the laser (*1*), was passed through a set of neutral light filters (*2*), which was necessary for the control of the radiation energy on the sample. The use of neutral light filters allowed more precise selection of the input energy ranges required for various experimental conditions. A Glan prism (*3*) was necessary for the fixed sample location experiment. It was used for the adjustment of
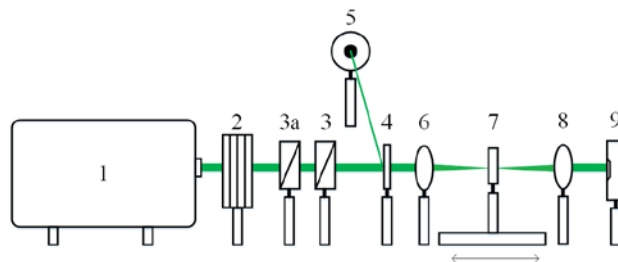

Fig. 2. Optical scheme of the experiment for detecting nonlinear optical absorption

Condensed Matter and Interphases / Конденсированные среды и межфазные границы   2021;23(4): 496–506

P. N. Vasilevsky et al.   Nonlinear optical properties of single-walled carbon nanotubes/water dispersed media...

laser radiation energy in ranges set by neutral light filters (*2*). Adjusting the energy values by rotating the Glan prism (*3*) can be carried out only when using polarized laser radiation, therefore, when working with a wavelength of 1064 nm, in front of the Glan control prism (*3*). A Glan polarizing prism (*3a*), transmitting only the linear polarization component, was additionally installed. When using radiation with a wavelength of 532 nm, polarization occurs in the laser during the generation of the second harmonic on a nonlinear crystal, therefore polarizing the Glan prism (*3a*) is not required.

Then the beam reached the beam splitter plate (*4*). It reflects ~ 5% of the original beam to the sensor (*5*), recording the input energy values. Lenses (*6*) and (*8*) have the same focal length *L* = 10 cm and are located confocal, at a distance of 2*L* = 20 cm. Due to this, the beam focused on the sample (*7*) by the lens (*6*), after passing through the lens (*8*) acquires the same shape as before focusing. The beam radius at the waist is 25 μm. A sample in a quartz cell with a thickness of 2 mm was placed on a motorized ruler, with which a Z-scan experiment was performed. Then the beam reached the sensor (*9*), which measured the values of the output energy, i.e. the energy after the passage of the beam through the sample.

Research was performed using Z-scan techniques and experiments with a fixed sample position. The radiation intensity was determined as:

$$I = \frac{2U}{\tau w^2 \pi^{3/2}},\tag{1}$$

where *U* – pulse energy, τ – pulse duration, *w* – the radius of the beam. In the case of a Z-scan, the intensity of the incident radiation changes by changing the radius of the beam. The radiation energy remains constant. For experiments with a fixed position of the sample, the investigated medium was placed in focus and the energy of the incident radiation changed.

1.3. Methods for determining nonlinear optical refraction

The study of the nonlinear refractive index was performed based on a femtosecond Ti:Sapphire laser Chameleon Ultra (Coherent, USA). The pulse generation frequency was 80 MHz, the pulse duration was 140 fs, and the wavelength was 800 nm. The lens focused the laser beam onto the studied sample. The focal length of the lens is 10 cm, the radius of the beam at the focus of the lens is 100 μm. For the reordering of the interference pattern obtained by spatial self-phase modulation, an SP620U CCD camera (Ophir, Israel) was placed behind the sample at a distance of 4 cm. For the limitation of the high-intensity laser radiation, a slit was used, which cut off part of the radiation with an increase in the beam radius. The experimental technique is similar to the experiment with a fixed position of the sample exposed to nanosecond radiation. The size of the slit was chosen in a way that the laser beam completely entered the hole in the absence of a sample. Irradiation was carried out when the cell was positioned vertically. The design of the experiment was similar to the experiment with a nanosecond laser, except for the presence of a slit and the absence of a second lens for collecting radiation.

3. Results and discussion

3.1. Linear and nonlinear optical properties under nanosecond radiation

The optical linear transmission spectrum of SWCNT/water dispersion in the range from 300 to 1100 nm is shown in Fig. 3. There were no pronounced peaks in the spectrum, with the exception of the water absorption peak in the wavelength range from 950 to 980 nm. The transmission at 532 and 1064 nm was 70%. In experiments with a nanosecond laser, the transmission of the medium with low radiation intensity, when nonlinear effects were not recorded, was also 70%. This suggests that the studied medium does not have colour selectivity, and the limiters created on the basis of such a medium will not cause colour discomfort during use. The linear absorption coefficient α was determined as:

$$\alpha(\lambda) = -\frac{\lg\left(T_{\text{lin}}(\lambda)\right)}{d}\tag{2}$$

where $T_{\text{lin}}(\lambda)$ – linear transmission at a certain wavelength, *d* – the thickness of the sample. In this study, a 2 mm thick cell was used in all experiments. For the 532 and 1064 nm wavelengths, the linear absorption coefficient α is 1.78.

Condensed Matter and Interphases / Конденсированные среды и межфазные границы   2021;23(4): 496–506

P. N. Vasilevsky et al.   Nonlinear optical properties of single-walled carbon nanotubes/water dispersed media...
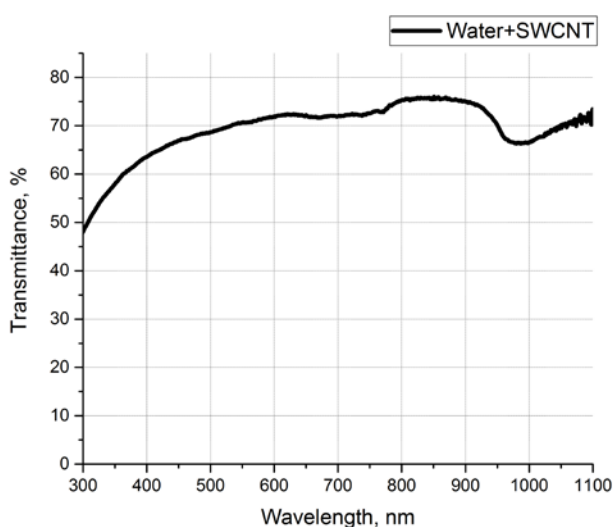

Fig. 3. Optical transmission spectrum of SWCNT/water dispersion

For the investigation of the nonlinear optical parameters of the studied medium interacting with pulsed nanosecond radiation, a cell with SWCNT/water dispersion was placed on a motorized linear positioner at a distance of 6 cm from the lens focus. A Z-scan experiment was then performed. The cell was moved along the optical axis of laser beam propagation and irradiated with single nanosecond pulse every 3 mm. The incident radiation energy remained unchanged and amounted to 550 mJ. Thus, we have obtained the dependence of the normalized transmission $T_{norm}(z)$ on the position of the test sample relative to the focus of the lens z, where $T_{norm}(z)$ is defined as:

$$T_{norm}\left(z\right) = \frac{T\left(z\right)}{T_{lin}}, \qquad (3)$$

where $T(z)$ – the transmission value at each point z, T_{lin} – the value of linear transmission, i.e. transmission in the absence of nonlinear effects.

Then the cell was placed in the focus of the lens, and the fixed sample location experiment was performed. Based on the results, the dependence of the energy of laser radiation transmitted through the sample on the energy of the radiation incident on the sample was obtained.

In Fig. 4 the experimental and theoretically calculated dependences for SWCNT/water dispersion at wavelengths of 532 nm (Fig. 4a, b) and 1064 nm (Fig. 4c, d). In Fig. 4a, it can be seen

that the decrease in the normalized transmission begins almost immediately after the start of the experiment. This indicates a low value of the threshold intensity for the studied medium at a wavelength of 532 nm. This also causes a narrow linear absorption zone in Fig. 4b. It can also be noted that in the presented dependencies there are no knock-out points that do not correspond to the general dependency. This indicates the high stability of the dispersion, i.e. the absence of large SWCNT agglomerates in it, which could contribute to a sharp change in the energy of the transmitted radiation and cause the limiter to malfunction. Also, post-focus transmittances correspond to pre-focus transmittances at similar distances. This shows that there were no changes in the medium (welding of individual nanotubes and precipitation, sublimation of SWCNT, formation of solvent microbubbles, etc.) when passing through the focus of the lens, i.e., through a region of high intensity.

A similar picture was observed upon pulsed irradiation of SWCNT/water dispersion at a wavelength of 1064 nm. As the cell approached the focus of the lens, a decrease in the normalized transmission and then the restoration of the optical properties the further from the focus were observed. In Fig. 4c, the linear absorption, region when the transmission of the medium did not change is clearly visible.

The onset of nonlinear absorption and the corresponding change in the characteristics of the medium can be described using the reverse saturable absorption mechanism and the Jablonski diagram [30]. With low laser radiation intensity, the absorption of photons causes the excitation of molecules from the ground state to the first excited state and is described by the Beer-Lamber-Bouguer law. As the intensity increases, the first excited state becomes almost completely occupied, and then the absorption is described by a transition from the first to the second excited state, i.e., it acquires a nonlinear character.

According to the results of experiments, the nonlinear optical parameters were calculated for SWCNT/water dispersion. The calculation of nonlinear optical parameters was carried out using a threshold model based on the radiation transfer equation [31]. This model allows taking into account the fact that changes
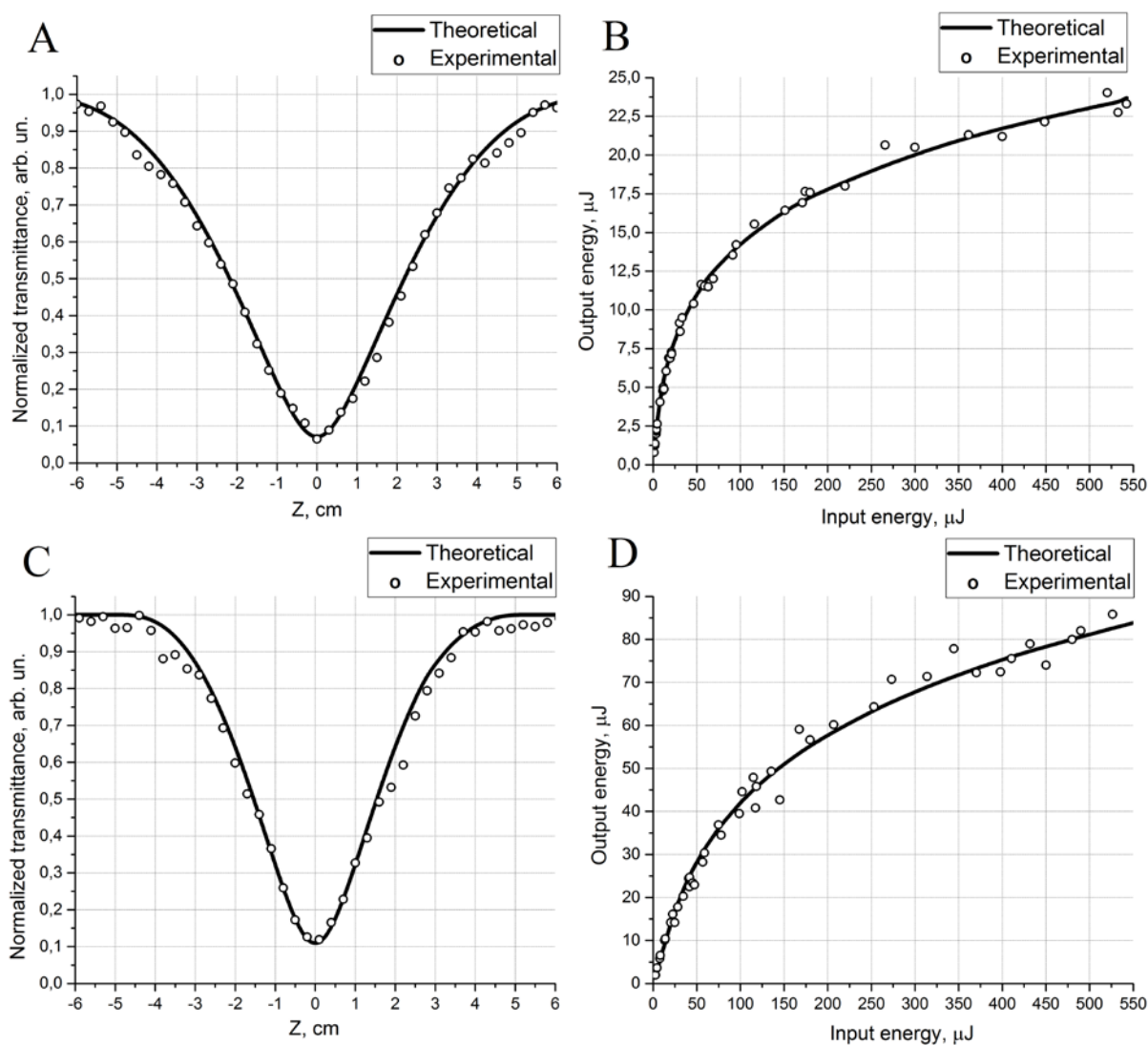
Condensed Matter and Interphases / Конденсированные среды и межфазные границы   2021;23(4): 496–506

P. N. Vasilevsky et al.   Nonlinear optical properties of single-walled carbon nanotubes/water dispersed media...

Fig. 4. Curves of dependences obtained from the results of Z-scanning and experiments with a fixed position of the sample for wavelengths of 532 (a, b) and 1064 nm (c, d)

in the parameters of the medium do not occur immediately, but only when a certain intensity value was reached:

$$\mu(I) = \alpha + \beta \cdot (I - I_{th}) \cdot \eta(I - I_{th}) \qquad (4)$$

where $\mu(I)$ - the total absorption coefficient, β – the nonlinear absorption coefficient, $\eta (I - I_{th})$ – Heaviside step function. Thus, after the calculation of the optical parameters presented in formula (4), it is possible to predict the behaviour of the medium under different intensities. The threshold model is described in detail in [32].

The calculation results are presented in Table 1. The difference in the threshold intensity can be explained by two-photon absorption. Although this effect is nonthreshold, it affects the degree of radiation absorption in addition to linear absorption. For this reason, gas formation can occur at the interface between the solid and liquid phases much earlier, which manifests as the formation of microbubbles and, accordingly, in an increase in absorption with an increase in the optical path of the laser beam due to multiple scattering [33]. Despite the higher nonlinear absorption coefficient, the attenuation coefficient at a wavelength of 1064 nm was lower than at a wavelength of 532 nm. This was due to the later occurrence of nonlinear absorption due to the higher threshold intensity. The values of the nonlinear absorption coefficient for SWCNT/water dispersion were much higher than the values for the graphene and graphene

Table 1. Optical parameters of SWCNT/water dispersion at different wavelengths

Wavelength, nm	Linear absorption coefficient, 1/cm	Nonlinear absorption coefficient, cm/GW	Threshold intensity, MW/cm^2	Attenuation coefficient
532	1.78	1111	5.5	15.3
1064	1.78	2010	18	9.7

oxide particles dispersions (3 and 45 cm/GW, respectively) presented in [34, 35]. This can be explained by the fact that carbon nanotubes increase multiple scattering more strongly, increasing the optical path inside the sample. Due to the increase in the optical path, more photons are absorbed, which causes more excitation in the molecules and, accordingly, stronger nonlinear properties.

3.2. Linear and nonlinear optical properties under femtosecond radiation

Irradiation with femtosecond radiation was performed in a frequency mode with a pulse repetition rate of 80 MHz. The cell was placed at the focus of the lens. Images from a CCD camera at different power of laser radiation are shown in Table 2. With low radiation power, the transmitted beam corresponds to the Gaussian shape of the incident beam. It can be seen that at the radiation power $P \approx 100$ mW the laser beam starts to expand significantly. The increase in power leads to the further expansion of the beam with the formation of a ring-shaped structure. The radius of the outer ring was taken as the beam size upon the formation of rings. It should be noted that the transmission of the sample in this case did not change with increasing power.

The emergence of such diffraction pattern is a consequence of spatial self-phase modulation [36]. The refractive index *n* starts to change due to the thermal effects in the medium, under the action of laser radiation above a certain threshold. In this case, due to the Gaussian shape of the incident radiation at different points of the medium, the change in the refractive index will be different, forming a gradient in the refractive index. This leads to the appearance of the self-defocusing effect, i.e., the divergence of the beam and an increase in its radius.

Together with this, a change in the phase of coherent laser radiation occurs in the medium, since a gradient change in the refractive index leads to a change in the propagation rate of the beam in the medium υ:
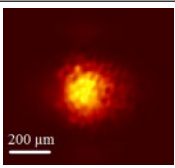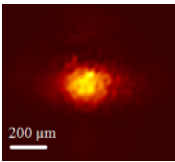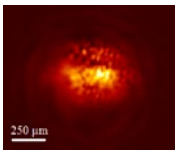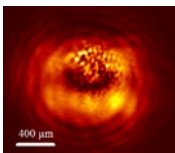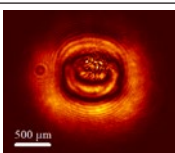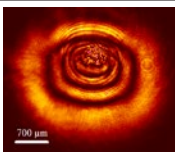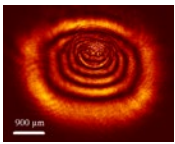
$$\upsilon = \frac{c}{n} \tag{5}$$

where *c* – the propagation rate of the beam in a vacuum. Thus, different parts of the transmitted radiation have different phases, which leads to the appearance of an interference pattern on the screen. Dark areas correspond to radiation in opposite phase, and light areas correspond to interference maxima.

The thermal nature of this effect was confirmed by the distortion of the interference pattern in the images. The rings above the centre of the irradiation site narrow, forming an asymmetry along the Y axis. This is due to the appearance of thermal convection determined by the vertical position of the cell. When the liquid is heated, the heat goes up, and the temperature gradient and the gradient of the refractive index, become smaller in the upper part of the irradiated zone. This leads to the approximately the same rate of beam propagation above the centre of irradiation and the phase shift becomes much lower the lower the centre of irradiation is or at the edges.

In our study, we propose to use the effect of spatial self-phase modulation to attenuate the power of radiation transmitted through the studied medium. For this, a system with a slit which cuts off part of the radiation at the expansion of beam was proposed. The dependence of the transmitted laser power on the incident power is shown in Fig. 5. It can be seen that when the power reached $P = 150$ mW, a sharp drop in the transmitted power occurred. This was due to the fact that the size of the beam becomes larger than the size of the slit, and part of the beam is cut off. With a further increase in the power, the transmitted power stops to decrease and again starts to increase slowly, but this increase was much less than in the linear case, i.e. before the appearance of a gradient in the

Condensed Matter and Interphases / Конденсированные среды и межфазные границы   2021;23(4): 496–506

P. N. Vasilevsky et al.   Nonlinear optical properties of single-walled carbon nanotubes/water dispersed media...

Table 2. The shape and size of the beam after passing through the sample at different powers

No.	Beam visualization from CCD camera	Power, mW	Beam size X, µm	Beam size Y, µm
1		10	280	280
2		45	270	220
3		100	500	300
4		160	1020	700
5		330	1880	1450
6		520	2700	2050
7		710	3600	2700

refractive index and the beam's expansion. Due to this transition from constant transmittance to nonlinear transmittance, the effect of limiting the power of laser radiation occurs. This effect can be used both for the protection of photosensitive elements and control of the signal in optical switches.

The value of linear refractive index n_0 was obtained using a portable refractometer. For the studied dispersion it was 1.33 and it was equal to the refractive index of water. This finding suggests that the addition of carbon nanotubes does not lead to a change in the refractive index of the solvent.

Based on the results of the experiment, the nonlinear refractive index n_2 was determined according to the formula:

$$n_2 = \frac{\lambda N}{2n_0 dI} = \frac{\lambda N w_0^2 \pi}{4n_0 dP},$$ (6)

where N - the number of rings. For the calculation, the number of rings was considered below the centre of irradiation. It was found that for the studied SWCNT/water dispersion sample, the nonlinear refractive index was 0.16 cm²/MW, which is several orders of magnitude higher than the nonlinear refractive index of graphene dispersion (0.0025 cm²/MW) obtained in [37]. A stronger non-linear

Condensed Matter and Interphases / Конденсированные среды и межфазные границы   2021;23(4): 496–506

P. N. Vasilevsky et al.   Nonlinear optical properties of single-walled carbon nanotubes/water dispersed media...
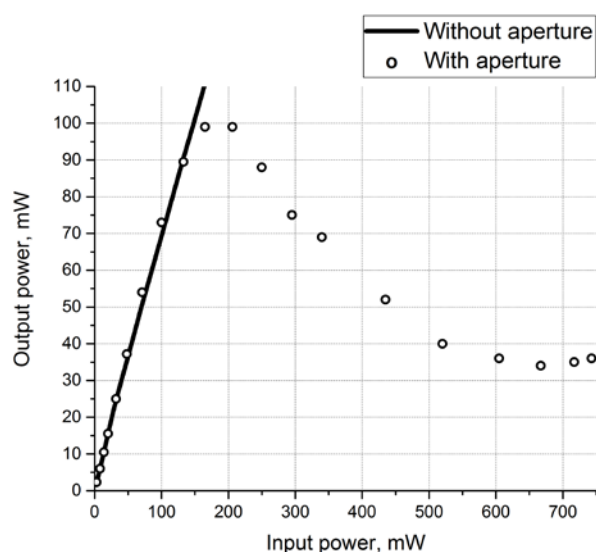

Fig. 5. Curve of the dependence of the transmitted power on the incident power when exposed to femtosecond radiation

response potentially leads to a larger increase in the radius of the rings, and thus a sharper decrease in transmission when using the slit.

4. Conclusions

As a result of the performed studies, the linear and nonlinear optical parameters for SWCNT/water dispersion at different wavelengths were determined. The obtained values can be used to characterize the investigated medium exposed to radiation of different intensities. The conditions for the occurrence of nonlinear absorption and refraction effects in a medium, leading to a change in the corresponding optical characteristics, were determined. The high stability of the investigated medium to the action of high-intensity laser radiation was shown. The effects of nonlinear absorption (reverse saturable absorption and two-photon absorption) and nonlinear refraction (spatial self-phase modulation) appear in the studied medium exposed to laser radiation with nano- and femtosecond pulse durations. The high linear transmission and the calculated nonlinear optical parameters allowed to conclude that SWCNT/water dispersion can be used for the limitation of both single pulses and radiation with a high pulse repetition rate in the visible and near IR ranges. Thus, single-walled carbon nanotubes have the potential to be used as an active medium of laser radiation limiters for the protection of light-sensitive sensors and visual organs.

Authors contributions

Vasilevsky P. N. – writing text, obtaining data for analysis, final conclusions. Savelyev M. S. – analysis of experimental data, development of methodology, text editing. Tereshchenko S. A. – creation of a theoretical model, text editing. Selishchev S.V. – research concept, text editing. Gerasimenko A. Yu. – scientific guidance, text editing.

Conflict of interests

The authors declare that they have no known competing financial interests or personal relationships that could have influenced the work reported in this paper.

References

1. Shin Y. C., Wu B., Lei S., Cheng G. J., Lawrence Yao Y. Overview of laser applications in manufacturing and materials processing in recent years. *Journal of Manufacturing Science and Engineering*. 2020;142(11): 110818. https://doi.org/10.1115/1.4048397

2. Kalisky Y. Y., Kalisky O. The status of high-power lasers and their applications in the battlefield. *Optical Engineering*. 2010;49(9): 091003. https://doi.org/10.1117/1.3484954

3. Nishizawa N. Ultrashort pulse fiber lasers and their applications. *Japanese Journal of Applied Physics*. 2014;53(9): 090101. http://dx.doi.org/10.7567/JJAP.53.090101

4. Kashaev N., Ventzke V., Çam G. Prospects of laser beam welding and friction stir welding processes for aluminum airframe structural applications. *Journal of Manufacturing Processes*. 2018;36: 571–600. https://doi.org/10.1016/j.jmapro.2018.10.005

5. Liaros N., Fourkas J. T. Ten years of two-color photolithography. *Optical Materials Express*. 2019;9(7): 3006–3020. https://doi.org/10.1364/OME.9.003006

6. Roberts H. W., Day A. C., O'Brart D. P. S. Femtosecond laser–assisted cataract surgery: a review. *European Journal of Ophthalmology*. 2020;30(3): 417–429. https://doi.org/10.1177/1120672119893291

7. Campbell P., Moore I. D., Pearson M. R. Laser spectroscopy for nuclear structure physics. *Progress in Particle and Nuclear Physics*. 2016;86: 127–180. https://doi.org/10.1016/j.ppnp.2015.09.003

8. Dekan M., František D., Andrej B., Jozef R., Dávid R., Josip M. Moving obstacles detection based on laser range finder measurements. *International Journal of Advanced Robotic Systems*. 2018;15(1): 1–18. https://doi.org/10.1177/1729881417748132

9. Bukin O. A., Babii M. Yu., Golik S. S., Il'in A. A., Kabanov A. M., Kolesnikov A. V., Kulchin Yu. N., Lisitsa V. V., Matvienko G. G., Oshlakov V. K.,

Condensed Matter and Interphases / Конденсированные среды и межфазные границы   2021;23(4): 496–506

P. N. Vasilevsky et al.   Nonlinear optical properties of single-walled carbon nanotubes/water dispersed media...

Shmirko K. A. Lidar sensing of the atmosphere with gigawatt laser pulses of femtosecond duration. *Quantum Electronics*. 2014;44(6): 563–569. https://doi.org/10.1070/QE2014v044n06ABEH015431

10. Goodin C., Carruth D., Doude M., Hudson C. Predicting the influence of rain on LIDAR in ADAS. *Electronics*. 2019;8(1): 89. https://doi.org/10.3390/electronics8010089

11. Farid N., Li C., Wang H., Ding H. Laser-induced breakdown spectroscopic characterization of tungsten plasma using the first, second, and third harmonics of an Nd: YAG laser. *Journal of Nuclear Materials*. 2013;433(1-3): 80–85. https://doi.org/10.1016/j.jnucmat.2012.09.002

12. Saylam K., Hupp J. R., Averett A. R., Gutelius W. F., Gelhar B. W. Airborne lidar bathymetry: assessing quality assurance and quality control methods with Leica Chiroptera examples. *International Journal of Remote Sensing*. 2018;39(8): 2518–2542. https://doi.org/10.1080/01431161.2018.1430916

13. Chomicki D., Kharchenko O., Skowronski L., Kowalonek J., Smokal V., Krupka O., Derkowska-Zielinska B. Influence of methyl group in a quinoline moiety on optical and light-induced properties of side-chain azo-polymers. *Applied Nanoscience*. 2021: 1–9. https://doi.org/10.1007/s13204-021-01764-0

14. Büyükekşi S. I., Karatay A., Orman E. B., Selçuki N. A., Özkaya A. R., Salih B., Elmali A., Şengül A. A novel AB 3-type trimeric zinc (ii)-phthalocyanine as an electrochromic and optical limiting material. *Dalton Transactions*. 2020;49(40): 14068–14080. https://doi.org/10.1039/D0DT02460K

15. Beverina L., Pagani G. A., Sassi M. Multichromophoric electrochromic polymers: colour tuning of conjugated polymers through the side chain functionalization approach. *Chemical Communications*. 2014;50(41): 5413–5430. https://doi.org/10.1039/C4CC00163J

16. Savelyev M. S., Gerasimenko A. Y., Vasilevsky P. N., Fedorova Y. O., Groth T., Ten G. N., Telyshev D. V. Spectral analysis combined with nonlinear optical measurement of laser printed biopolymer composites comprising chitosan/SWCNT. *Analytical biochemistry*. 2020;598: 113710. https://doi.org/10.1016/j.ab.2020.113710

17. Eevon C., Halimah M. K., Zakaria A., Azurahanim C. A. C., Azlan M. N., Faznny M. F. Linear and nonlinear optical properties of Gd^{3+} doped zinc borotellurite glasses for all-optical switching applications. *Results in Physics*. 2016;6: 761–766. https://doi.org/10.1016/j.rinp.2016.10.010

18. Varma S. J., Kumar, J., Liu, Y., Layne, K., Wu, J., Liang, C., Nakanishi Y., Aliyan A. Yang W. Ajayan P. M., Thomas J. 2D TiS_2 layers: a superior nonlinear optical limiting material. *Advanced Optical Materials*. 2017;5(24): 1700713. https://doi.org/10.1002/adom.201700713

19. Tutt L. W., Boggess T. F. A review of optical limiting mechanisms and devices using organics, fullerenes, semiconductors and other materials. *Progress in Quantum Electronics*. 1993;17(4): 299–338. https://doi.org/10.1016/0079-6727(93)90004-S

20. Li R., Dong N., Ren F., Amekura H., Wang J., Chen F. Nonlinear absorption response correlated to embedded Ag nanoparticles in BGO single crystal: from two-photon to three-photon absorption. *Scientific Reports*. 2018;8(1): 1–8. https://doi.org/10.1038/s41598-018-20446-6

21. Miao R., Hu Y., Ouyang H., Tang Y., Zhang C., You J., Zheng X., Xu Z., Cheng X., Jiang T. A polarized nonlinear optical response in a topological insulator Bi_2Se_3–Au nanoantenna hybrid-structure for all-optical switching. *Nanoscale*. 2019;11(31): 14598–14606. https://doi.org/10.1039/C9NR02616A

22. Savelyev M. S., Vasilevsky P. N., Gerasimenko A. Y., Ichkitidze L. P., Podgaetsky V. M., Selishchev S. V. Nonlinear optical characteristics of albumin and collagen dispersions with single-walled carbon nanotubes. *Materials Physics and Mechanics*. 2018;37(2): 133–139. https://doi.org/10.18720/mpm.3722018_4

23. Savotchenko S. E. Periodic states near the plane defect with non-linear response separating non-linear self-focusing and linear crystals. *Kondensirovannye Sredy I Mezhfaznye Granitsy = Condensed Matter and Interphases*. 2020;20(2): 255–262. https://doi.org/10.17308/kcmf.2018.20/517

24. Valligatla S., Haldar K. K., Patra A., Desai N. R. Nonlinear optical switching and optical limiting in colloidal CdSe quantum dots investigated by nanosecond Z-scan measurement. *Optics & Laser Technology*. 2016;84: 87–93. https://doi.org/10.1016/j.optlastec.2016.05.009

25. Zhang Y., Wang Y. Nonlinear optical properties of metal nanoparticles: a review. *RSC Advances*. 2017;7(71); 45129–45144. https://doi.org/10.1039/C7RA07551K

26. Kuzmina E. A., Dubinina T. V., Vasilevsky P. N., Saveliev M. S., Gerasimenko A. Y., Borisova N. E., Tomilova L. G. Novel octabromo-substituted lanthanide (III) phthalocyanines–Prospective compounds for nonlinear optics. *Dyes and Pigments*. 2021;185: 108871. https://doi.org/10.1016/j.dyepig.2020.108871

27. Papagiannouli I., Bourlinos A. B., Bakandritsos A., Couris S. Nonlinear optical properties of colloidal carbon nanoparticles: nanodiamonds and carbon dots. *RSC Advances*. 2014;4(76): 40152–40160. https://doi.org/10.1039/C4RA04714A

28. Gerasimenko A. Yu. Laser structuring of the carbon nanotubes ensemble intended to form biocompatible ordered composite materials. *Kondensirovannye Sredy I Mezhfaznye Granitsy = Condensed Matter and Interphases*. 2017;19(4): 489–

Condensed Matter and Interphases / Конденсированные среды и межфазные границы   2021;23(4): 496–506

P. N. Vasilevsky et al.   Nonlinear optical properties of single-walled carbon nanotubes/water dispersed media...

501. https://doi.org/10.17308/kcmf.2017.19/227 (In Russ., absract in Eng.)

29. Atlukhanova L. B., Dolbin I. V., Kozlov G. V. The Physics of Interfacial Adhesion between a Polymer Matrix and Carbon Nanotubes (Nanofibers) in Nanocomposites. *Kondensirovannye Sredy I Mezhfaznye Granitsy = Condensed Matter and Interphases*. 2020;22(2): 190–196. https://doi.org/10.17308/kcmf.2020.22/2822

30. Maurya S. K., Rout A., Ganeev R. A., Guo C. Effect of size on the saturable absorption and reverse saturable absorption in silver nanoparticle and ultrafast dynamics at 400 nm. *Journal of Nanomaterials*. 2019;2019: 1–13. https://doi.org/10.1155/2019/9686913

31. Tereshchenko S. A., Podgaetskii V. M., Gerasimenko A. Yu., Savel'ev M. S. Threshold effect under nonlinear limitation of the intensity of high-power light. *Quantum Electronics*. 2015;45(4): 315–320. https://doi.org/10.1070/QE2015v045n04ABEH015569

32. Tereshchenko S. A., Savelyev M. S., Podgaetsky V. M., Gerasimenko A. Yu., Selishchev S. V. Nonlinear threshold effect in the Z-scan method of characterizing limiters for high-intensity laser light. *Journal of Applied Physics*. 2016;120(9): 093109. https://doi.org/10.1063/1.4962199

33. Savelyev M. S., Gerasimenko A. Y., Podgaetskii V. M., Tereshchenko S. A., Selishchev S. V., Tolbin A. Y. Conjugates of thermally stable phthalocyanine J-type dimers with single-walled carbon nanotubes for enhanced optical limiting applications. *Optics & Laser Technology*. 2019;117: 272–279. https://doi.org/10.1016/j.optlastec.2019.04.036

34. Tong Q., Wang Y. H., Yu X. X., Wang B., Liang Z., Tang M., Wu A. S., Zhang H. J., Liang F., Xie Y. F. Nonlinear optical and multi-photon absorption properties in graphene–ZnO nanocomposites. *Nanotechnology*. 2018;29(16): 165706. https://doi.org/10.1088/1361-6528/aaac13

35. Wang S., Dong Y., He C., Gao Y., Jia N., Chen Z., Song W. The role of sp 2/sp 3 hybrid carbon regulation in the nonlinear optical properties of graphene oxide materials. *RSC Advances*. 2017;7(84): 53643–53652. https://doi.org/10.1039/C7RA10505C

36. Li J., Zhang Z., Yi J., Miao L., Huang J., Zhang J., He Y., Huang B., Zhao C., Zou Y., Wen S. Broadband spatial self-phase modulation and ultrafast response of MXene $Ti_3C_2T_x$ (T= O, OH or F). *Nanophotonics*. 2020;9(8): 2415–2424. https://doi.org/10.1515/nanoph-2019-0469

37. Stavrou M., Dalamaras I., Karampitsos N., Couris S. Determination of the nonlinear optical properties of single-and few-layered graphene dispersions under femtosecond laser excitation: electronic and thermal origin contributions. *The Journal of Physical Chemistry C*. 2020;124(49): 27241–27249. https://doi.org/10.1021/acs.jpcc.0c09959

Information about the authors

Pavel N. Vasilevsky, Postgraduate Student, Engineer in Institute of Biomedical Systems, National Research University of Electronic Technology – MIET, Zelenograd, Moscow, Russian Federation; Junior Research Fellow, Institute of Nanotechnology of Microelectronics of the Russian Academy of Sciences, Moscow, Russian Federation; e-mail: pavelvasilevs@yandex.ru. ORCID iD: https://orcid.org/0000-0002-5733-8497.

Mikhail S. Savelyev, PhD in Physics and Mathematics, Assistant Professor in Institute of Biomedical Systems, National Research University of Electronic Technology – MIET, Zelenograd, Moscow, Russian Federation; Research Fellow, Institute of Nanotechnology of Microelectronics of the Russian Academy of Sciences, Moscow, Russian Federation; Research Fellow, I. M. Sechenov First Moscow State Medical University, Moscow, Russian Federation; e-mail: savelyev@bms.zone. ORCID iD: https://orcid.org/0000-0003-1255-0686.

Sergey A. Tereshchenko, DSc in Physics and Mathematics, Professor in Institute of Biomedical Systems, National Research University of Electronic Technology – MIET, Zelenograd, Moscow, Russian Federation; Research Fellow, Institute of Nanotechnology of Microelectronics of the Russian Academy of Sciences, Moscow, Russian Federation; e-mail: tsa@miee.ru. https://orcid.org/0000-0002-3163-5741.

Sergey V. Selishchev, DSc in Physics and Mathematics, Director of Institute of Biomedical Systems, National Research University of Electronic Technology – MIET, Zelenograd, Moscow, Russian Federation; e-mail: selishchev@bms.zone. ORCID: https://orcid.org/0000-0002-5589-7068.

Alexander Yu. Gerasimenko, Dsc in Physics and Mathematics, Assistant Professor in Institute of Biomedical Systems, National Research University of Electronic Technology – MIET, Zelenograd, Moscow, Russian Federation; Research Fellow, Institute of Nanotechnology of Microelectronics of the Russian Academy of Sciences, Moscow, Russian Federation; Head of the Laboratory of Biomedical Nanotechnology, I. M. Sechenov First Moscow State Medical University, Moscow, Russian Federation; e-mail: gerasimenko@bms.zone. https://orcid.org/0000-0001-6514-2411.